ELSEVIER

Physica A 273 (1999) 231–240

PHYSICA A

www.elsevier.com/locate/physa

Post-deposition island growth with long-range interactions

Oana Tataru[a,*], Fereydoon Family[a], Jacques G. Amar[b]

[a] *Department of Physics, Emory University, Atlanta, GA 30322, USA*

[b] *Department of Physics and Astronomy, University of Toledo, OH 43606, USA*

Received 23 June 1999

Abstract

The effects of long-range interactions on the scaling of the average island-size, island-size distribution, and saturation time are investigated for a simple model of post-deposition island growth. While long-range interactions are found to have little effect on the scaled island-size distribution, the average island-size is strongly affected. Excellent agreement is found with the proposed scaling form $S(\theta,t)=\theta^z g(\theta t^\beta)$ for the average island size $S(\theta,t)$ at time t and coverage θ. The exponents z and β and the scaling function $g(u)$ depend on the range and sign of the interaction. Long-range interactions are also found to strongly affect the saturation time as well as the exponent describing its dependence on coverage. This leads to a simple experimental method to detect the presence of long-range interactions. © 1999 Elsevier Science B.V. All rights reserved.

PACS: 81.15.Aa; 68.35.-p; 68.35.Bs; 68.35.Fx

1. Introduction

Molecular-beam epitaxy (MBE) is an important technique used to grow thin films, high-quality crystals, nanostructures and a variety of other semiconductor and magnetic materials. In the early stages of growth, the main processes that play a role are the deposition and diffusion of adatoms and the formation and growth of islands by nucleation, aggregation and coalescence [1–3]. Understanding how the island density and island size-distribution are influenced by these atomic-scale competing processes is an essential first step in describing thin-film growth.

One of the key parameters affecting the island-density and size distribution in submonolayer epitaxial growth is the ratio D/F of the adatom hopping rate D to the

* Corresponding author. Fax: +1-404-727-0873.

E-mail address: otataru@emory.edu (O. Tataru)

PII: S0378-4371(99)00276-9

deposition rate F, which is typically much larger than 1. Accordingly, a great deal of recent theoretical [4–16] and experimental [17–27] work has focussed on the dependence of these quantities on the ratio D/F as well as on the critical island size i corresponding to one less than the number of atoms in the smallest stable cluster. However, in some cases, i.e. at relatively low temperatures and large deposition fluxes, this ratio may be quite small. In this case, which we refer to as post-deposition nucleation, island nucleation and growth occur primarily after deposition has occurred rather than during deposition. Accordingly, in this regime the primary factors affecting the island-density and distribution are the total coverage deposited (θ) and the critical island size as well as the length of time after deposition.

Recently, the submonolayer scaling behavior in post-deposition nucleation has been studied using point-island [28] as well as more realistic extended-island models [29]. These studies have been motivated by several thin-film growth experiments [30–32] in which the flux of adatoms is shut off and the surface is either annealed at a somewhat higher temperature, or simply allowed to relax before a subsequent layer is deposited. All of these studies have assumed the existence of short-range interactions such as nearest-neighbor bonding. However, in the presence of Coulomb effects or elastic effects due to strain, long-range interactions may occur. Depending on the signs of the interactions these long-range interactions may be either attractive or repulsive. Accordingly, in the present work we present simulation results for post-deposition nucleation with both attractive and repulsive long-range interactions. We note that recently there have been experimental and theoretical studies [33,34] of the deposition of charged clusters on a surface buffer layer in the absence of nucleation.

2. Model and simulations

To study the effects of long-range interactions, kinetic Monte Carlo simulations were carried out using a model of post-deposition nucleation which includes a long-range interaction of the form $V(r) = V_0/r$, where $V_0 > 0$ corresponds to a repulsive interaction and $V_0 < 0$ corresponds to an attractive interaction between diffusing particles. In addition to the long-range interaction, a much stronger short-range interaction, corresponding to irreversible attachment of adatoms to nearest-neighbor atoms or clusters was included, so that atoms with at least one nearest-neighbor bond are "frozen". This corresponds to low-temperature deposition and a critical island size of $i = 1$. For comparison, post-deposition nucleation without long-range interactions [29] was also studied.

In our simulations we assumed that deposition takes place on a two-dimensional square lattice of adsorption sites of lateral size L with periodic boundary conditions. In order to model the initial rapid deposition, a finite fraction θ of the L^2 lattice sites were randomly occupied. Atoms without nearest-neighbor bonds (monomers) were then allowed to diffuse on the square-lattice under the influence of the long-range interaction until every atom was a member of a cluster, i.e. had at least one nearest-neighbor bond. The hopping rate D was taken to be the same for all monomers. This is a good approximation since the long-range interaction was assumed to be relatively weak. However, due to the long-range interactions, the probability p_i for a given monomer to hop in any one of the four possible directions of motion was assumed to depend on the direction and on the long-range interaction in the following way,

$$p_i = \frac{e^{-\delta V_i/k_B T}}{\sum_i e^{-\delta V_i/k_B T}} , \tag{1}$$

where the subscript i corresponds to one of the four directions for hopping on a square lattice, and δV_i corresponds to the change in the long-range interaction energy $V(r)$ corresponding to motion in that direction. In the case of long-range attraction the coupling constant ($V_0/k_B T = -8.63$) was chosen such that the probability of hopping towards an isolated monomer two lattice constants away is ten times larger than the probability of hopping away. Similarly, in the case of long-range repulsion the repulsion strength ($V_0/k_B T$=4.12) was chosen such that a particle two lattice constants away from an isolated monomer is three times more likely to hop away from the monomer than towards the monomer. In our simulations we assumed a cutoff radius R_0 which was chosen such that for two isolated monomers separated by a distance R_0 the difference in the hopping probability towards or away from each other was less than 5%. Since this choice of R_0 also corresponded to a distance significantly larger than the correlation length, then by symmetry we expect that the influence of particles beyond this range will be negligible.

In order to study the dynamical behavior, the average island size $S(\theta,t) = (\theta - n_1(\theta,t))/n(\theta,t)$, where $n(\theta,t)$ is the number density of islands per lattice site and $n_1(\theta,t)$ is the monomer density, was measured for different coverages as a function of time t, where $t=0$ just after deposition (i.e. at the start of the nucleation process). In addition, the island-size distribution $n_s(\theta)$, where n_s is the density per site of islands of size s, was measured at saturation when all monomers have been incorporated in islands. In order to obtain good statistics, simulations were carried out using periodic boundary conditions on lattices of size $L = 128$ and 256 and were averaged over 1000 runs.

3. Scaling of the island-size distribution and average island size

In our analysis of the island-size distribution $n_s(\theta)$ we assumed the standard scaling form [9,14],

$$n_s(\theta) = \theta S^{-2} f\left(\frac{s}{S}\right), \quad s \geqslant 2 , \tag{2}$$

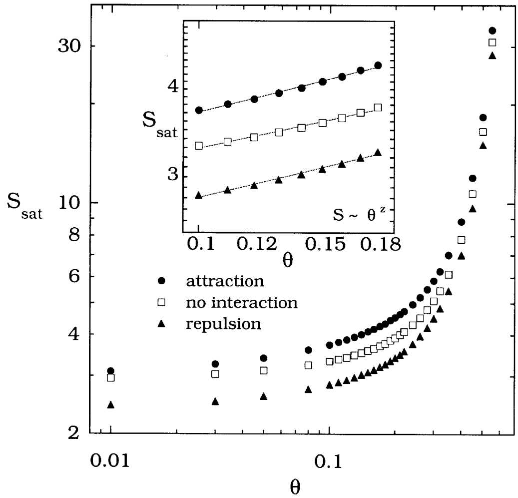

Fig. 1. Variation of the average island size with coverage in the saturated regime for the three types of interaction (attraction, no interaction, repulsion) is plotted for a wide range of coverages. The inset shows the same quantities plotted over a range of coverages for which the assumption $S(\theta) \sim \theta^z$ is more realistic.

where the scaling function $f(u)$ is assumed to be independent of coverage. The use of this scaling form is based on the assumption that there is only one relevant length-scale or size corresponding to the average island size.

In order to study the dependence of the average island size $S(\theta, t)$ on both time t and coverage θ, we propose a dynamic scaling expression of the form,

$$S(\theta, t) \sim \theta^z g(\theta t^\beta) , \tag{3}$$

where $g(u) \sim u^\delta$ for $u \ll 1$ and $g(u) \sim$ *constant* for $u \gg 1$. At early times ($u \ll 1$) this implies $S(\theta, t) \sim \theta^\omega t^\gamma$ where $\omega = z + \delta$ and $\gamma = \beta\delta$.

4. Results

Fig. 1 shows our results for the dependence of the average island size at saturation $S(\theta)$ on coverage for all three cases studied: attractive long-range interaction, repulsive long-range interaction and no long-range interaction. As can be seen, attraction leads to a larger average island size than in the absence of long-range interactions while repulsion leads to a smaller average island size. The increase in $S(\theta)$ for the case of attractive interaction is due to the increased number of aggregation events at the expense of nucleation, as the monomers are attracted toward nearby islands. Conversely, for the case of a long-range repulsive interaction, the island-monomer repulsion leads to an increase in the monomer density and a resulting increase in the nucleation rate thus increasing the number of islands and decreasing the average island size at

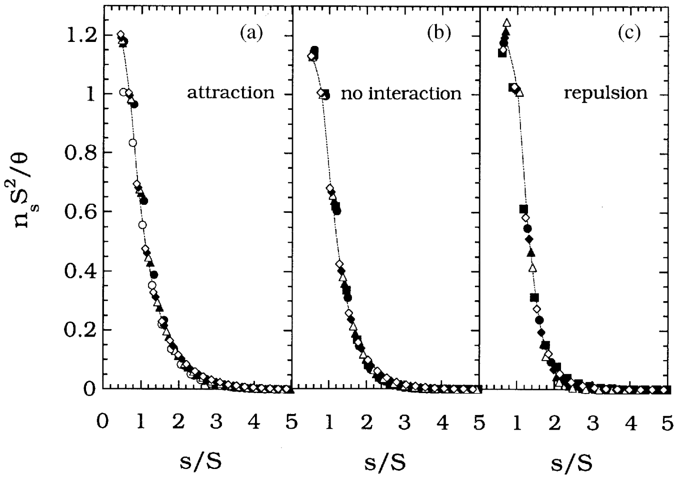

Fig. 2. Scaled island-size distribution for $0.1 < \theta < 0.2$ for (a) attraction, (b) no interaction and (c) repulsion.

saturation. While the long-range interaction strongly affects the average island-size and island-density the effect on the exponent z describing the coverage-dependence of S is much weaker. At low coverage this is not surprising since the distances between adatoms are comparable to the interaction radius R_0 and thus there are only a few actual long-range interaction events. At the other limit for high coverages, many adatoms are located within each adatom's interaction range and their interaction effects cancel out leading to an almost random motion. The inset shows the coverage-dependence of the saturated island size $S(\theta)$ on θ over a typical range of coverage studied experimentally ($\theta = 0.1$–0.2). Over this coverage range the effective exponent z (which is equal to 0.22 in the absence of interaction) is increased to 0.26 and 0.28 for the case of attractive and repulsive interaction, respectively. These results indicate that even though attraction and repulsion have opposite effects on the average island-size, they both lead to increased values for the effective dynamic exponent z. This is due to the enhanced sensitivity of the saturated island size on coverage in the presence of long-range interactions.

Fig. 2 shows the scaled island-size distribution $f(s/S) = n_s(\theta)S^2/\theta$ at saturation over the same range of coverages ($\theta = 0.1$–0.2). As can be seen there is good scaling in all three cases. Note that the shape of the distribution is only weakly affected by the long-range interaction. Thus, while the presence of a long-range interaction strongly affects the nucleation rate and average island size, it has almost no effect on the scaled island-size distribution.

We now consider the coverage and time dependence of the average island-size $S(\theta, t)$ at low coverage and early time. As can be seen in Figs. 3–5 there is excellent scaling using the form $S(\theta, t) \sim \theta^z g(\theta t^\beta)$ both in the absence of long-range interaction as well as for attractive and repulsive interactions. The dynamical exponents ω and γ increase (decrease) with the degree of long-range attraction (repulsion). The exponent

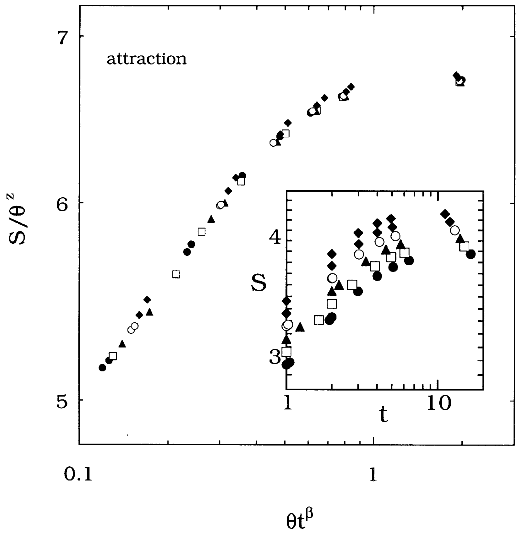

Fig. 3. Scaled island size S/θ^z as a function of θt^β for the case of long-range attraction ($\beta = 1.0, z = 0.26$). Inset shows unscaled data.

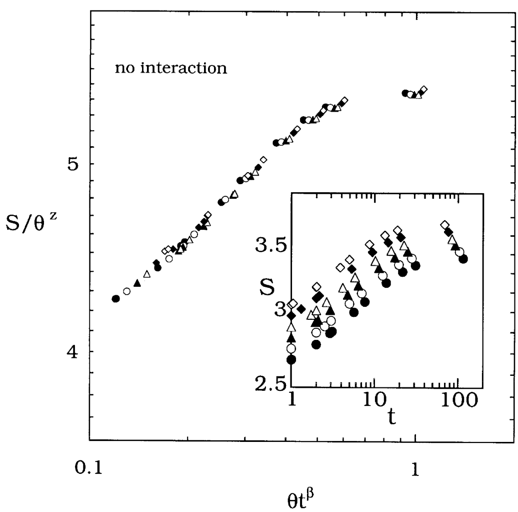

Fig. 4. Scaled island size S/θ^z as a function of θt^β for the case of no interaction ($\beta = 0.43, z = 0.22$). Inset shows unscaled data.

$\beta = \gamma/(\omega - z)$ was calculated by first determining the values for γ and ω. By fitting $S(\theta, t \to 0) = \theta^{\omega} t^{\gamma}$, at early times as a function of coverage and time, we obtained $\gamma_r = 0.008$, $\gamma_0 = 0.06$, and $\gamma_a = 0.16$ and $\omega_r = 0.32$, $\omega_0 = 0.36$, and $\omega_a = 0.42$ where the subscripts $r, 0$, and a refer to repulsion, no interaction, and attraction, respectively.

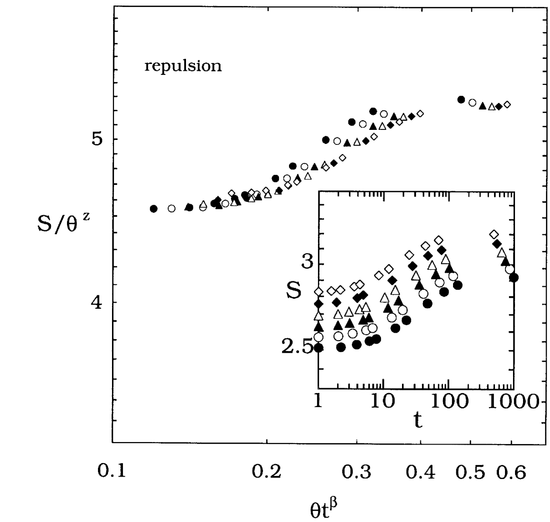

Fig. 5. Scaled island size S/θ^z as a function of θt^β for the case of long-range repulsion ($\beta = 0.2, z = 0.28$). Inset shows unscaled data.

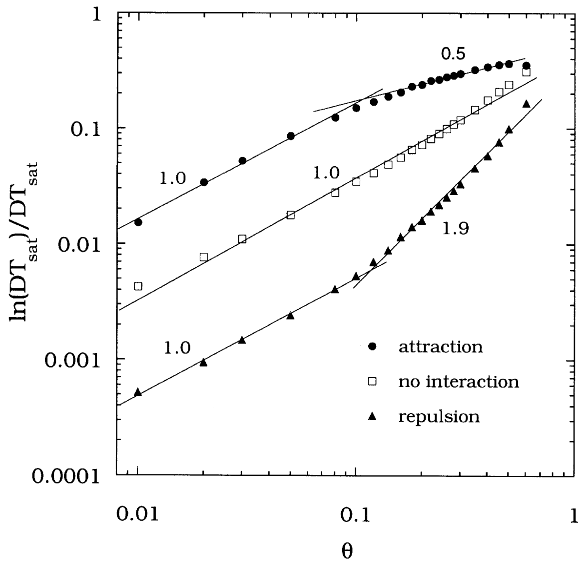

Fig. 6. Log–log plot of $\ln(T_{sat})/T_{sat}$ versus coverage θ for long-range attraction, no interaction and long-range repulsion.

Finally, we consider the dependence of the saturation time T_{sat}, corresponding to the time after deposition is completed until only stable islands are left, on the deposition coverage θ. For the non-interacting case we find $\ln(DT_{sat})/DT_{sat} \sim \theta$ as shown in Fig. 6. This result may be explained by considering the number of distinct sites $v(t)$

visited by a two-dimensional random walk in two-dimensions after Dt hops, which satisfies [35],

$$v(t) \sim \frac{Dt}{\ln(Dt)} . \tag{4}$$

To reach the final state, when all particles belong to stable islands, each particle should on average visit a number of sites of order $1/\theta$, before encountering another particle or cluster. This implies that we can write an expression relating the total time of the monomer diffusion process and the coverage:

$$\frac{\ln(DT_{sat})}{DT_{sat}} \sim \theta^x , \tag{5}$$

where $x = 1$ in the absence of long-range interactions.

As can be seen in Fig. 6, the saturation time T_{sat} is significantly smaller for the case of attraction than for the non-interacting case since $\ln(DT_{sat})/(DT_{sat})$ is significantly larger. Similarly, the saturation time is significantly larger for the case of long-range repulsion than for the non-interacting case. The long-range interactions also lead to a change in the exponent x describing the dependence of T_{sat} on θ for $\theta > 0.1$. In particular, over the coverage range $0.1 < \theta < 0.2$ we find $x < 1$ for the case of attraction and $x > 1$ for the case of repulsion. The decrease in x for the case of attraction is due to the fact that a monomer visits fewer sites in this case before attaching to another monomer or cluster. Similarly, for the case of repulsion, a monomer must visit a larger number of sites on average before attaching to another monomer or island so that $x > 1$. Thus, we find that the scaling of the saturation time T_{sat} as a function of θ is strongly affected by the existence of long-range interactions. These results indicate a simple way to determine the presence of long-range interactions experimentally by measuring the exponent x describing the dependence of the saturation time on coverage during post-deposition island growth.

5. Conclusions

Using kinetic Monte Carlo simulations we have investigated the effects of both long-range attractive and repulsive interactions on post-deposition nucleation. Our results indicate that while the scaled island-size distribution is not strongly affected, the average island size is strongly affected by the presence of long-range interactions. In particular, the average island-size at saturation was found to be significantly larger in the presence of long-range attraction and significantly smaller in the presence of long-range repulsion than in the absence of long-range interactions. In addition, the scaling exponent z describing the dependence of saturated island size on coverage was found to be somewhat enhanced in the presence of long-range interactions.

We also studied the dynamic scaling behavior of the average island size as a function of coverage during the early stages of the post-deposition nucleation process. We found excellent agreement with the scaling form $S = \theta^z g(\theta t^\beta)$ in all three cases. The exponents z and β were found to depend on the presence of the long-range interaction. Finally, we studied the dependence of the saturation time T_{sat} on coverage. For the non-interacting case, we found excellent agreement with a simple scaling theory for the dependence of T_{sat} on coverage. For the case of long-range interaction a similar scaling form was observed but with an exponent x which depended on the sign of the interaction. In particular, for the case of long-range attraction T_{sat} was significantly smaller than in the non-interacting case, while in the case of long-range repulsion it was significantly larger. In addition, the exponent x describing the dependence of T_{sat} on coverage was found to be significantly different in the interacting case than in the non-interacting case at intermediate coverage. These results suggest a simple experimental method to look for the effects of long-range interactions by studying the dependence of the saturation time on coverage during post-deposition nucleation.

References

[1] F. Family, J.G. Amar, in “Dynamics of Fluctuating Interfaces and Related Phenomena”, D. Kim, H. Park, B. Kahng (Eds.), World Scientific, Singapore, 1997, p. 206.
[2] Z. Zhang, M.G. Lagally, Science 276 (1997) 377.
[3] F. Family, Physica A 266 (1999) 173.
[4] P. Smilauer, M.R. Wilby, D.D. Vvedensky, Phys. Rev. B 47 (1993) 4119.
[5] G.S. Bales, D.C. Chrzan, Phys. Rev. B 50 (1994) 6057.
[6] J.G. Amar, F. Family, P.M. Lam, Phys. Rev. B 50 (1994) 8781.
[7] J.G. Amar, F. Family, Phys. Rev. Lett. 74 (1995) 2066.
[8] A.F. Voter, Phys. Rev. B 34 (1986) 6819.
[9] T. Vicsek, F. Family, Phys. Rev. Lett. 52 (1984) 1669.
[10] J.A. Blackman, P. Mulheran, Phys. Rev. B 54 (1996) 11 681.
[11] L.-H. Tang, J. Phys. I 3 (1993) 935.
[12] F. Family, P. Meakin, Phys. Rev. A 40 (1989) 3836.
[13] F. Family, P. Meakin, Phys. Rev. Lett. 61 (1988) 428.
[14] M.C. Bartelt, J.W. Evans, Phys. Rev. B 46 (1992) 12 675.
[15] M.C. Bartelt, J.W. Evans, Phys. Rev. B 54 (1996) 17 359.
[16] M.C. Bartelt, J.W. Evans, Surf. Sci. 298 (1993) 421.
[17] R.Q. Hwang, J. Schroder, C. Gunther, R.J. Behm, Phys. Rev. Lett. 67 (1991) 3279.
[18] J.A. Stroscio, D.T. Pierce, Phys. Rev. B 49 (1994) 8522.
[19] J.A. Stroscio, D.T. Pierce, R.A. Dragoset, Phys. Rev. Lett. 70 (1993) 3615.
[20] D.D. Chambliss, K.E. Johnson, Phys. Rev. B 50 (1994) 5012.
[21] H.J. Ernst, F. Fabre, J. Lapujoulade, Phys. Rev. B 46 (1992) 1929.
[22] H.-N. Yang, G.-C. Wang, T.-M. Lu, Phys. Rev. Lett. 73 (1994) 2348.
[23] J.-K. Zuo, J.F. Wendelken, Phys. Rev. Lett. 66 (1991) 2227.
[24] J.-K. Zuo, J.F. Wendelken, H. Durr, C.-L. Liu, Phys. Rev. Lett. 72 (1994) 3064.
[25] Y.W. Mo, J. Kleiner, M.B. Webb, M.G. Lagally, Phys. Rev. Lett. 66 (1991) 1998.
[26] W. Li, G. Vidali, O. Biham, Phys. Rev. B 48 (1993) 8336.
[27] M. Zinke-Allmang, S.C. Puddephatt, T.D. Lowes, Epitaxial Growth Process. SPIE 2140 (1994) 36.
[28] J. Li, A.G. Rojo, L.M. Sander, Phys. Rev. Lett. 78 (1997) 1747.
[29] O. Tataru, J.G. Amar, F. Family, preprint.
[30] Y. Okada, J.S. Harris Jr., A. Sutoh, M. Kawabe, Mater. Res. Soc. Symp. Proc. 399 (1996) 203.
[31] R. Kunkel, B. Poelsema, L.K. Verheij, G. Comsa, Phys. Rev. Lett. 65 (1990) 733.

[32] G. Rosenfeld, R. Servaty, C. Teichert, B. Poelsema, G. Comsa, Phys. Rev. Lett. 71 (1993) 895.
[33] J. Wendelken, W.-W. Pai, Z. Zhang, to be published.
[34] M.-C. Chang, Z. Zhang, to be published.
[35] J. Villain, A. Pimpinelli, L. Tang, D. Wolf, J. Phys. I 2 (1992) 2107.